Spin-polarization reversal at the interface between benzene and Fe(100)

Souraya Goumri-Said, Mohammed Benali Kanoun, Aurélien Manchon, and Udo Schwingenschlögl

Citation: Journal of Applied Physics **113**, 013905 (2013); doi: 10.1063/1.4772610
View online: http://dx.doi.org/10.1063/1.4772610
View Table of Contents: http://scitation.aip.org/content/aip/journal/jap/113/1?ver=pdfcov
Published by the AIP Publishing

Spin-polarization reversal at the interface between benzene and Fe(100)

Souraya Goumri-Said,[1,a)] Mohammed Benali Kanoun,[2,b)] Aurélien Manchon,[1] and Udo Schwingenschlögl[1,c)]
[1]*PSE Division, KAUST, Thuwal 23955, Saudi Arabia*
[2]*KAUST Catalysis Center (KCC), KAUST, Thuwal 23955-6900, Saudi Arabia*

(Received 18 November 2012; accepted 29 November 2012; published online 3 January 2013)

The spin-polarization at the interface between Fe(100) and a benzene is investigated theoretically using density functional theory for two positions of the organic molecule: planar and perpendicular with respect to the substrate. The electronic and magnetic properties as well as the spin-polarization close to the Fermi level strongly depend on the benzene position on the iron surface. An inversion of the spin-polarization is induced by *p-d* hybridization and charge transfer from the iron to the carbon sites in both configurations. © *2013 American Institute of Physics*.
[http://dx.doi.org/10.1063/1.4772610]

I. INTRODUCTION

The study of spin phenomena in organic materials, coined as Organic Spintronics,[1] has gained increasing attention in the past few years with the realization of spin-selective organic devices. Organic-based spin-valves have been fabricated using various spacers, such as T_6 (Ref. 2) (sexithienyl), Alq_3 (tris-(8-hydroxyquinoline)aluminum),[3–6] or rubrene,[7,8] inserted between magnetic layers, such as the magnetic oxides $(La, Sr)MnO_3$, transition metals, or organic magnets. The major interest in organic materials comes from their low cost, light weight, as well as their probable long spin diffusion length.[8]

A significant challenge to obtain efficient organic spin-selective devices is the efficiency of the spin injection from the ferromagnetic material into the organic spacer. The complex nature of organic/inorganic ferromagnetic interfaces has been emphasized in recent publications.[4,5,9–11] In particular, the specific chemical bonding between the adsorbed organic molecule and the ferromagnetic surface is expected to dramatically influence the polarization of the injected electrons. For instance, the spin polarization at the Co/Alq_3 and $(La, Sr)MnO_3/Alq_3$ interfaces has been found positive in Ref. 5, whereas it is found negative in $NiFe/Alq_3$. Recent scanning tunneling microscopy experiments have also reported strong energy-dependent polarization reversal at the interface between Fe and organic rings (benzene, cyclopentadienyl radical, and cyclooctatetraene).[12] Several models have been proposed to explain the observed polarization reversal: the presence of an electrical dipolar moment,[4] the broadening of the interfacial states,[5] and p_z-d orbital overlap.[12] Although this spin polarization reversal has also been observed in inorganic junctions, such as $Co/SrTiO_3/(La, Sr)MnO_3$,[13] the mechanisms involved are likely to be different due to the nature of the organic molecule. An accurate understanding of this mechanism is necessary to control the organic spin-valve efficiency.

In this paper, we theoretically investigate the electronic structure of the interface between Fe(100) and a benzene molecule (C_6H_6). It is found that the interfacial magnetic properties and spin-polarization are controlled by the hybridization between the d orbitals of Fe and the p orbitals of the molecule. In particular, a spin polarization reversal is observed, attributable to the charge transfer between the metallic surface and the molecule.

II. COMPUTATIONAL DETAILS

In interfacial studies, the accurate description of the optimal physisorption of the organic molecule on the metallic surface is crucial. A key step is the definition of the potentials (by the force field) to study the gas-solid interaction, followed by the geometry optimization. In order to avoid the difficulties encountered when treating van der Waals systems with density functional theory,[14,15] we use molecular mechanics which can be seen as a precursor to computationally more expensive quantum mechanical methods.[16] In order to evaluate the role of orbital hybridization in the electronic structure of the interface, the C_6H_6 molecule is placed in two configurations: planar and perpendicular to the Fe(100) surface. Once the model has been optimized with the Forcite code[17,18] including vdW interactions between the aromatic molecule and the surface, the electronic structure of the $C_6H_6/Fe(100)$ interface is determined using density functional theory within the full-potential (linearized) augmented plane waves plus local orbitals method as implemented in WIEN2k.[19]

The $C_6H_6/Fe(100)$ system is modeled by a slab supercell approach with a $p(5 \times 6)$ flat surface. The supercell contains 6 atomic layers with a single adsorbed benzene molecule on one side of the slab and a vacuum layer of 20 Å, avoiding interactions between the periodically repeated images. The (100) surface is generated using the theoretical lattice parameters calculated for bulk iron (2.866 Å). After the structure optimization, we find that all six C-C bonds in the benzene molecule are of the same length (1.418 Å), which is longer than a double bond (1.35 Å) but shorter than a single bond (1.47 Å). This intermediate distance is consistent with

[a)]Souraya.Goumri-Said@kaust.edu.sa.
[b)]Mohammed.Kanoun@kaust.edu.sa.
[c)]Udo.Schwingenschlogl@kaust.edu.sa.

the experimental data and also with the electron delocalization: The valence electrons are distributed equally between the six C atoms.[20] The bond angles remain almost exactly 30°. Beyond, the optimized shortest distances between the ring C atoms and the first layer of the surface are: 1.36 Å, 1.40 Å, 1.68 Å, 1.74 Å, 1.97 Å, and 1.99 Å.

The exchange and correlation effects are treated within the Perdew-Burke-Ernzerhof generalized gradient approximation.[21] Basis functions are expanded simultaneously as spherical harmonic functions (inside non-overlapping muffin-tin (MT) spheres centred at atomic sites) and as plane waves in the interstitial region. The l-expansion (azimuthal quantum number) of the non-spherical potential and charge density inside the MT spheres is carried out up to $l_{max} = 10$. In order to achieve energy eigenvalue convergence, the wave functions in the interstitial region are expanded in plane waves with a cutoff of $K_{max} = 7/R_{MT}$ (where, K_{max} is the maximum modulus of the reciprocal lattice vectors and R_{MT} is the smallest of all MT sphere radii). Moreover, local orbitals are added for all atoms and valence states. The MT radii for Fe, C, and H are chosen to be 1.75, 1.35, and 0.9 atomic units, respectively. The self-consistency cycle is based on 10 points in the irreducible Brillouin zone. Convergence is ensured with respect to the energy and density.

III. RESULTS AND DISCUSSION

Local spin-resolved densities of states (LDOS) of the d states of an iron atom of the clean surface and of Fe atoms next to the planar and perpendicular benzene molecules are displayed in Figs. 1(a)–1(c), respectively. We notice important differences between these three graphs, which can be attributed to the hybridization between the d orbitals of Fe and the p orbitals of benzene, displayed in Figs. 2(a) and 2(b). In the case of the in-plane ring position, the hybridization involves all the p orbitals and even s orbitals, see Fig. 2(a). Therefore, the p-d hybridization is stronger in the planar configuration than in the perpendicular configuration. In the case of the perpendicular position, the hybridization is mainly of p_z-$d_{3z^2-r^2}$ type in the energy interval $[-1, 0]$ of

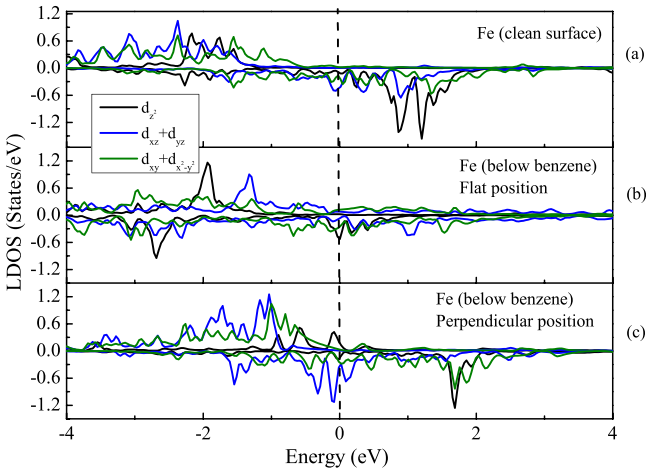

FIG. 1. Spin-resolved local density of states of Fe in the clean surface (upper panel), the Fe atom below C for the in-plane position (medium panel) and for the perpendicular position (lower panel).

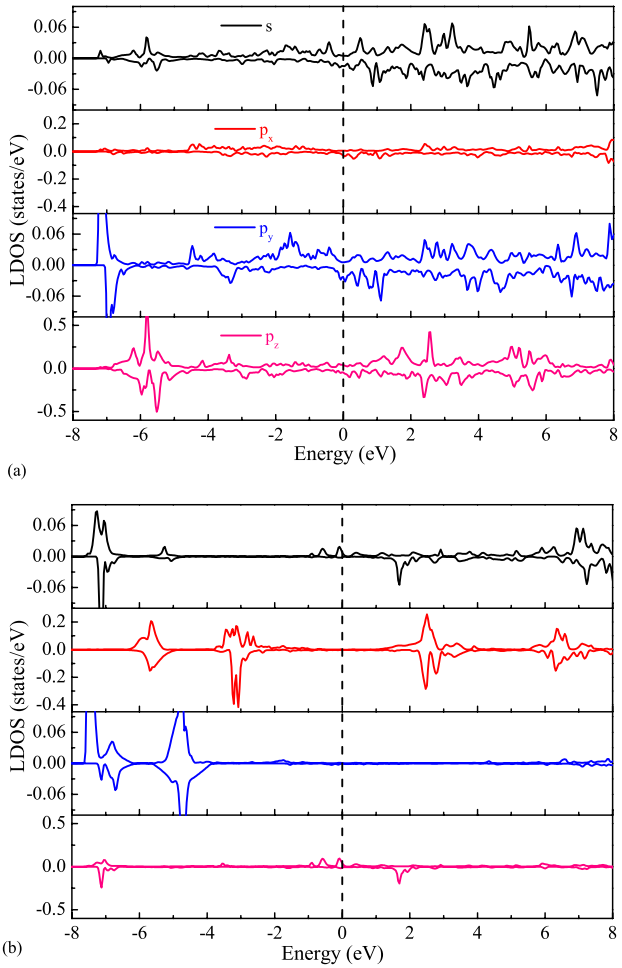

FIG. 2. Spin-resolved local density of states of a selected C atom. (a) Planar ring benzene and (b) perpendicular ring benzene.

Fig. 2(b). Note in Fig. 2(a), the $d_{3z^2-r^2}$ surface state of the Fe(001) surface at an energy of 0.23 eV.

This difference in the hybridization strength is reflected by the induced magnetic moment of the benzene ring. In the case of the planar position, the magnetic moment is about 0.032 μ_B for the C atoms of the benzene ring and 1.30 μ_B for the Fe atoms located underneath. For comparison, an average magnetic moment of 1.98 μ_B is found for the rest of the Fe atoms of the substrate. Therefore, bringing the benzene ring to the Fe surface induces a slight magnetization of the benzene molecule, accompanied by a decrease in the magnetization of the Fe atoms located underneath. In the perpendicular case, only one C atom is in contact with the surface and therefore develops a magnetic moment (0.026 μ_B).

Most interestingly, the polarization of the DOS at the Fermi energy is also strongly affected by the presence of the benzene molecule. This quantity is of major interest for spin-injection experiments. Although the spin-polarization P is energy-dependent (see, e.g., Ref. 12), we only consider the polarization of the DOS at the Fermi energy (E_F), defined as $P = \frac{N_\uparrow(E_F) - N_\downarrow(E_F)}{N_\uparrow(E_F) + N_\downarrow(E_F)}$, where $N_\sigma(E_F)$ is the total DOS for spin σ ($\sigma = \uparrow$ for majority electrons and $\sigma = \downarrow$ for minority). Using the DOSs in Figs. 2(a) and 2(b), we find $P = +0.35$ for the planar case and $P = +0.47$ for the perpendicular case. These values are opposite to the spin-polarization of the clean

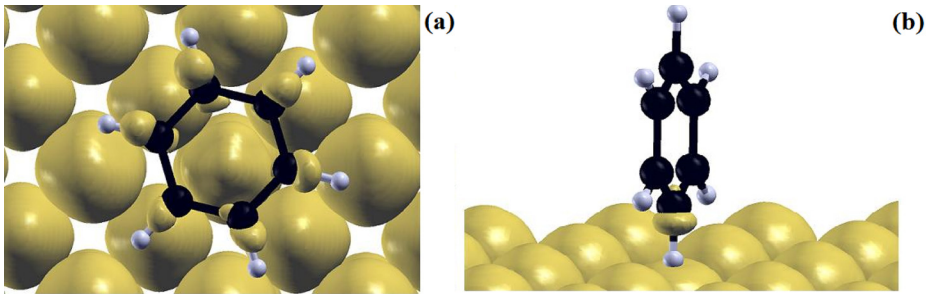

FIG. 3. Spin-density iso-surface plot for (a) planar ring benzene and (b) perpendicular ring benzene.

surface ($P = -0.47$), which indicates that the aromatic molecule inverses the carrier polarization. We will show that the change in the sign of the spin-polarization at the Fermi energy is related to the *p-d* hybridization mentioned above.

In order to consolidate these results, we plot the spin-density iso-surfaces for both cases in Figs. 3(a) and 3(b). It is clear that the spin-polarization of the benzene originates from the interaction of the molecule with the magnetic Fe surface. The spherical shape of the spin-density iso-surface of the Fe atom situated below the ring is deformed as compared to the rest of the Fe atoms. The planar molecule shows a net magnetic moment distributed over the molecule plane in contrast to the perpendicular case. Furthermore, the presence of a large number of *p* electrons in the planar case, see the DOS, causes an amplification of the magnetization of the ring as hybrid states of Fe *d* and C *p* orbitals are formed. In the perpendicular case, the spin-down p_z orbitals are lowered in energy and slightly hybridized with the minority *d* states of Fe. These results confirm the calculation recently performed by Atodiresei *et al.*,[12] where the authors suggest that the mechanism explaining the hybridization at the interface is similar to the well known p_z-*d* Zener exchange mechanism[22] observed in diluted magnetic semi-conductors.[23,24]

In order to examine the characteristics of the bonding and interaction of the benzene with the Fe surface, which may be considered as a representative magnetic metal surface, we present in Figs. 4(a) and 4(b) charge density contour plots. When we compare the isolated benzene to the plots including the Fe surface, we observe that the charge density increases slightly in the central region between the benzene and the substrate. This increase is related to the transfer of charge between the molecule and the iron layer underneath. Even though charge distribution is still more localized at the molecule, there is some charge transfer to the first layer of the Fe surface from the ring (yellow color on Fe sites) and to the center of the molecule, see the green curve in Fig. 4(b). In Fig. 4(c), we display a three dimensional-isosurface plot of the valence charge, where the isosurface around the π ring of the benzene and the thin "bridge" between benzene and the substrate indicate the donation of electrons from the aromatic adsorbate to the Fe substrate.[25] This result confirms the peak in the p_z LDOS in the energy range around -6 eV in Fig. 2(a). The same applies to the perpendicular benzene position, where a similar peak is observed, around -7 eV, for the p_z orbitals of the unique C atom bound to the Fe substrate (see Fig. 2(b)). Consequently, the interaction between

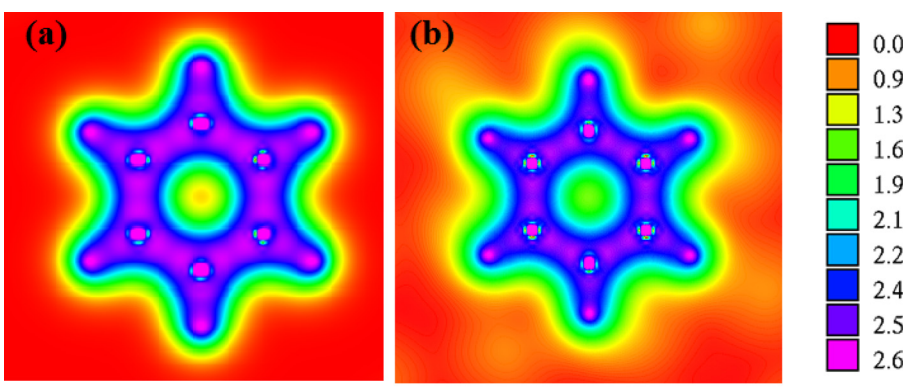

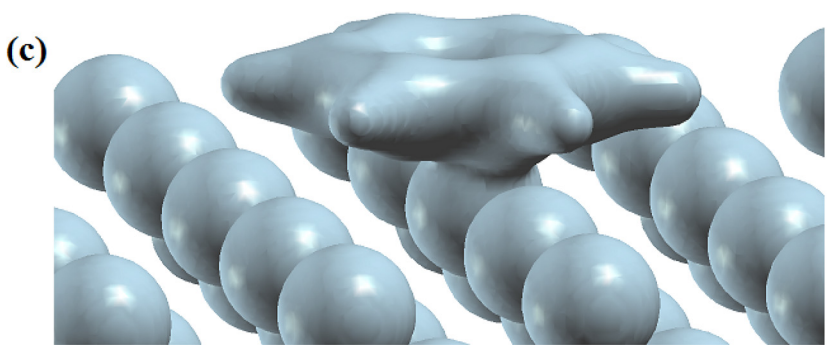

FIG. 4. Valence charge density for the planar ring. (a) Isolated C_6H_6 and ((b) and (c)) benzene/Fe(100) interface.

the aromatic adsorbate and the magnetic surface causes significant electron donation and backdonation, similar to the case of Pentacene/Fe(100).[26,27] This leads to the previously mentioned peaks of the carbon atoms bound to Fe and the filling of the π^* states of the C_6H_6. We conclude that the increases of the charge density on the Fe below the ring may be related to the polarization of the ring induced by the magnetic Fe.

IV. SUMMARY

In summary, the spin-polarized electronic structure of a benzene molecule adsorbed on a Fe(100) surface was investigated by first-principles calculations, considering planar and perpendicular positions of the aromatic molecule. Although the adsorbed molecule is nonmagnetic, a spin-polarization induced by the ferromagnetic surface is observed. The local density of states of the benzene/Fe(100) interface provides support of an inversion of the spin-polarization close to the Fermi level. The spin-polarization process is governed by two mechanisms: *p-d* Zener exchange and charge transfer from Fe to C atoms. The inversion of the spin-polarization is controlled by the position and distance of the aromatic molecule with respect to the ferromagnetic surface.

[1]V. A. Dediu, L. E. Hueso, I. Bergento, and C. Taliani, Nature Mater. **8**, 707 (2009).
[2]V. Dediu, M. Murgia, F. C. Matacotta, C. Taliani, and S. Barbanera, Solid State Commun. **122**, 181 (2002).
[3]Z. H. Xiong, D. Wu, Z. Valy Vardeny, and J. Shi, Nature **427**, 821 (2004).
[4]L. Schulz, L. Nuccio, M. Willis, P. Desai, P. Shakya, T. Kreouzis, V. K. Malik, C. Bernhard, F. L. Pratt, N. A. Morley, A. Suter, G. J. Nieuwenhuys, T. Prokscha, E. Morenzoni, W. P. Gillin, and A. J. Drew, Nature Mater. **10**, 3944 (2011).
[5]C. Barraud, P. Seneor, R. Mattana, S. Fusil, K. Bouzehouane, C. Deranlot, P. Graziosi, L. Hueso, I. Bergenti, V. Dediu, F. Petroff, and A. Fert, Nat. Phys. **6**, 615 (2010).
[6]D. Sun, L. Yin, C. Sun, H. Guo, Z. Gai, X.-G. Zhang, T. Z. Ward, Z. Cheng, and J. Shen, Phys. Rev. Lett. **104**, 236602 (2010).
[7]J.-W. Yoo, C.-Y. Chen, H. W. Jang, C. W. Bark, V. N. Prigodin, C. B. Eom, and A. J. Epstein, Nature Mater. **9**, 638 (2010); B. Li, C.-Y. Kao, J.-W. Yoo, V. N. Prigodin, and A. J. Epstein, Adv. Mater. **23**, 3382 (2011).
[8]J. H. Shim, K. V. Raman, Y. J. Park, T. S. Santos, G. X. Miao, B. Satpati, and J. S. Moodera, Phys. Rev. Lett. **100**, 226603 (2008).
[9]M. Cinchetti, K. Heimer, J.-P. Wüstenberg, O. Andreyev, M. Bauer, S. Lach, C. Ziegler, Y. Gao, and M. Aeschlimann, Nature Mater. **8**, 115 (2009).
[10]A. J. Drew, G. Szulczewski, L. Nuccio, and W. P. Gillin, Phys. Status Solidi B **249**, 9 (2012).
[11]P. Ruden, Nature Mater. **10**, 8 (2011); S. Sanvito, Nat. Phys. **6**, 562 (2010).
[12]N. Atodiresei, J. Brede, P. Lazić, V. Caciuc, G. Hoffmann, R. Wiesendanger, and S. Blügel, Phys. Rev. Lett. **105**, 066601 (2010); J. Brede, N. Atodiresei, S. Kuck, P. Lazic, V. Caciuc, Y. Morikawa, G. Hoffmann, S. Blügel, and R. Wiesendanger, Phys. Rev. Lett. **105**, 047204 (2010).
[13]J. M. De Teresa, A. Barthélémy, A. Fert, J. P. Contour, R. Lyonnet, F. Montaigne, P. Seneor, and A. Vaurés, Phys. Rev. Lett. **82**, 4288 (1999).
[14]S. J. Jenkins, Proc. R. Soc. A **465**, 2949 (2009).
[15]N. Atodiresei, V. Caciuc, P. Lazić, and S. Blügel, Phys. Rev. Lett. **102**, 136809 (2009).
[16]F. Rosei, M. Schunack, Y. Naitoh, P. Jiang, A. Gourdon, E. Laegsgaard, I. Stensgaard, C. Joachim, and F. Besenbacher, Prog. Surf. Sci. **71**, 95 (2003), and references therein.
[17]Forcite code is implemented in MATERIALS STUDIO, Version 5.2.5, Accelrys Inc., San Diego, CA, 2009.
[18]For simulations that use forcefields, the interactions of a system of particles are governed by an analytic expression that represents the potential energy surface, the energy expression. For large systems, the energy expression can consist of many terms and so the Forcite code provides an automated way of constructing it. Key elements of this construction are the forcefield type (potential type) and the (forcefield) atom type.
[19]P. Blaha, K. Schwarz, G. K. H. Madsen, D. Kvasnicka, and J. Luitz, *WIEN2k: An Augmented Plane Wave + Local Orbitals Program for Calculating Crystal Properties* (Vienna University of Technology, Vienna, Austria, 2001).
[20]D. Moran, A. C. Simmonett, F. E. Leach, W. D. Allen, P. V. R. Schleyer, and H. F. Schaefer, J. Am. Chem. Soc. **128**, 9342 (2006).
[21]J. P. Perdew, K. Burke, and M. Ernzerhof, Phys. Rev. Lett. **77**, 3865 (1996).
[22]T. Dietl, Semicond. Sci. Technol. **17**, 377 (2002).
[23]M. B. Kanoun, S. Goumri-Said, A. E. Merad, and J. Cibert, J. Phys. D: Appl. Phys. **38**, 1853 (2005).
[24]T. Dietl, H. Ohno, F. Matsukura, J. Cibert, and D. Ferrand, Science **287**, 1019 (2000).
[25]X. Sun, Y. Yamauchi, M. Kurahashi, T. Suzuki, Z. P. Wang, and S. Entani, J. Phys. Chem. C **111**, 15289 (2007).
[26]H. P. Steinrück, W. Huber, T. Pache, and D. Menzel, Surf. Sci. **218**, 293 (1989).
[27]X. Sun, T. Suzuki, Y. Yamauchi, M. Kurahashi, Z. P. Wang, and S. Entani, Surf. Sci. **602**, 1191 (2008).